frontiers in Materials

ORIGINAL RESEARCH
published: 15 January 2021
doi: 10.3389/fmats.2020.591281

Photothermal Therapy Based on CuS Nanoparticles for Alleviating Arterial Restenosis Induced by Mechanical Injury of Endovascular Treatment

Xiaoyu Wu[1], Kun Liu[1], Qun Huang[1], Qin Zhang[2], Xinrui Yang[1]*, Xiaobing Liu[1]* and Ruihua Wang[1]**

[1]Department of Vascular Surgery, Shanghai Ninth People's Hospital, Shanghai Jiao Tong University School of Medicine, Shanghai, China, [2]Institute of Translational Medicine, Shanghai University, Shanghai, China

OPEN ACCESS

Edited by:
Guanjie He,
University of Lincoln, United Kingdom

Reviewed by:
Jingyi Zhu,
Nanjing Tech University, China
Shilei Ni,
Jilin University, China
Yong Gao,
The First Affiliated Hospital of Bengbu Medical College, China

***Correspondence:**
Qin Zhang
sabrina_1985@shu.edu.cn
Xinrui Yang
Cinder_13@126.com
Xiaobing Liu
benny_liuxb@163.com
Ruihua Wang
wangruihua0330@sina.com

Specialty section:
This article was submitted to Biomaterials, a section of the journal Frontiers in Materials

Received: 04 August 2020
Accepted: 12 October 2020
Published: 15 January 2021

Citation:
Wu X, Liu K, Huang Q, Zhang Q, Yang X, Liu X and Wang R (2021) Photothermal Therapy Based on CuS Nanoparticles for Alleviating Arterial Restenosis Induced by Mechanical Injury of Endovascular Treatment. Front. Mater. 7:591281. doi: 10.3389/fmats.2020.591281

CuS nanoparticles (NPs) as an effective near-infrared absorption agent have been widely applied in the photothermal therapy (PTT) of cancer. However, little is known about the application of CuS NP-based PTT in alleviating arterial inflammation and restenosis, which affects the long-term prognosis of endovascular treatment. In this study, CuS NPs were synthesized and used as PTT nanoplatform for ameliorating arterial inflammation induced by mechanical injury of endovascular treatment. The macrophages possess powerful phagocytosis toward CuS NPs is evidenced by intracellular transmission electron microscopic imaging. As illustrated from Cell Counting Kit-8 assay and calcein AM/PI staining, an efficient depletion of macrophages by CuS NPs coculture combined with the irradiation with a 915-nm near-infrared laser was achieved. The endarterium injury/inflammation model was established by insertion of a 29G needle (BD Insulin Syringe Ultra-Fine®) to the left common carotid artery of an apolipoprotein E knockout mouse to mimic endarterium damage after endovascular treatment. Local injection of CuS NPs around the left common carotid artery followed by irradiation with a 915-nm INR laser significantly depleted infiltrated macrophages and alleviated arterial stenosis. This work emphasizes the role of CuS NPs as a PTT agent in post-injury remodeling of the arterial wall and provides an attractive target macrophage that can be depleted to alleviate arterial restenosis.

Keywords: CuS nanoparticles, computed tomography, photothermal therapy, arterial restenosis, macrophage

INTRODUCTION

Atherosclerosis obliterans of the extracranial carotid artery accounts for 15–20% of ischemic strokes (Li et al., 2015). Combination of percutaneous transluminal angioplasty and stent implantation has become alternative to endarterectomy partly because it has the advantages of shorter operation time, less invasion, and quick recovery (Beckman et al., 2020). Regardless of refinements of the endovascular technique, the mechanical injury to the endarterium is unavoidable, and subsequent arterial inflammation and restenosis are still incompletely understood and entirely unpredictable or unpreventable (Hong and Lee, 2020).

The negative remodeling of the arterial wall mediated by arterial inflammation is a hallmark of restenosis (Williams et al., 2019). Mechanical injury of endovascular treatment wrecks the integrity and continuity of the endarterium, which triggers the release of a number of cytokines from

endothelial cells, neutrophils, and platelets (Arakawa et al., 2005) and recruits massive circulating monocytes to the arterial intima (Koelwyn et al., 2018). Via serious signaling pathways (Tong et al., 2020), recruited monocytes differentiate into macrophages, which mediates the chronic inflammation of the injured artery (Koelwyn et al., 2018). After penetrating into the lesion site, macrophages contribute to the secretion of matrix metalloproteinase to degrade the extracellular matrix and release of pro-inflammatory chemokines to stimulate the transformation and proliferation of smooth muscle cells, ultimately leading to arterial restenosis (Jinnouchi et al., 2020; Tong et al., 2020). Thus, depletion of abnormal infiltrated macrophages provides novel insights into alleviating restenosis after endovascular treatment.

Photothermal therapy (PTT) using nanoparticles as near-infrared (NIR) absorption agents has been widely applied in medicine, especially cancer therapy (Wang et al., 2020). The principal mechanism of its therapeutic effect is converting light energy into thermal energy, which results in degeneration of DNAs and proteins of target cells (de Melo-Diogo et al., 2017). Taking advantage of this feature, we have effectively developed this procedure using $CuCo_2S_4$ nanocrystals (Zhang et al., 2019), MoO_2 nanoclusters (Wang et al., 2019), polypyrrole nanoparticles (Peng et al., 2015), and gold nanorods (Qin et al., 2015) to alleviate arterial inflammation by eliminating macrophages. As typical semiconductor materials, copper chalcogenides, especially CuS NPs, have many unique advantages as new photothermal conversion materials owing to strong NIR absorbance, photostability, and low toxicity (Zhou et al., 2010; Cheng et al., 2014; Yang et al., 2016). With strong absorption in the NIR (700–1,400 nm), copper chalcogenides were first reported as photothermal reagents by Li et al. (2000), who found that thioglycolate-coated copper sulfide nanoparticle exhibited good laser-induced photothermal effect in eliminating cancer cells. CuS NPs, nanoplatforms with dual photoacoustic/magnetic resonance imaging, and PTT are being widely studied in the anticancer field (Poudel et al., 2019). *In vivo* experiments confirmed evident accumulation of CuS NPs with both imaging and therapeutic functions in breast cancer, and cancer growth was inhibited markedly through synergistic photodynamic/PTT (Zhou et al., 2010; Hu X. et al., 2020). Despite wide utilization of copper-based nanoparticle–based PTT on cancer treatment with promising results, it is currently unknown whether PTT using CuS NPs as NIR absorption reagent can ameliorate negative remodeling of arterial wall that is, restenosis after endovascular treatment by eliminating artery infiltrating macrophages.

Toward this end, CuS NPs were synthesized, and their characterization and photothermal properties were measured. The cytotoxicity and PTT effect on macrophages were evaluated *in vitro*. The endarterium injury/inflammation model was established by insertion of a 29G needle (BD Insulin Syringe Ultra-Fine®) to the left common carotid artery of the apolipoprotein E knockout mouse to mimic endarterium damage after endovascular treatment. PTT therapy based on the local administration of CuS NPs was subsequently carried out. Of note, we specially evaluated the imaging property of CuS NPs for *in vivo* tracking by small animal CT device. Histopathological examination was conducted to assess the effect of PTT in alleviating arterial restenosis. This work emphasized the novelty of CT-guided therapy based on CuS NPs in prevention and treatment of arterial restenosis after mechanical injury of the endarterium.

MATERIALS AND METHODS

Materials

$CuCl_2$, sodium citrate, and Na_2S were purchased from Sinopharm Chemical Reagent Co., Ltd. (Shanghai, China) and used without purification. Mouse macrophage cell line, Raw 264.7, was purchased from the Beijing Cell Bank, the Chinese Academy of Medical Sciences (Beijing, China). Dulbecco's modified Eagle's medium (DMEM, with high glucose 4,500 mg ml^{-1}), fetal bovine serum, trypsin-EDTA (0.25%), and penicillin/streptomycin were purchased from Thermo Fisher (New York, United States). The primary CD68 antibody and relevant second antibody were purchased from Thermo Fisher (New York, United States). The Cell Counting Kit-8 (CCK-8) and Calcein-AM/PI Double Stain Kit were purchased from Dojindo (Kumamoto, Japan).

Synthesis of CuS Nanoparticles

The CuS NPs were synthesized according to the method described previously (Zhou et al., 2010). To 1,000 ml of aqueous solution of sodium citrate (0.2 g, 0.68 mmol) and $CuCl_2$ (0.1345 g, 1 mmol), 1 ml of sodium sulfide solution (Na_2S, 1 M) was added under magnetic stirring at room temperature. Ten minutes later, the mixture was heated to 90°C and stirred until dark green color appeared, and then the mixture was transferred to ice-cold water. The Cit-CuS NPs were obtained and stored at 4°C for further use.

Characterization of CuS Nanoparticles

Scanning electron microscopy (JEM-2010F; Japan) was used to determine the size, microstructure, and morphological properties of the CuS NPs. X-ray diffractometer analysis was conducted on a BT-X X-ray diffractometer (Olympus, Tokyo, Japan). UV-vis absorption spectra and diffuse reflectance spectra were recorded by using a TP720 UV-vis-NIR spectrophotometer (Olympus, Tokyo, Japan) from 400 to 1,000 nm. Fourier transform infrared spectra were measured by using KBr pellet methods using an infrared spectrometer (IRPrestige-21; Japan). Contents of ions released from the synthesized CuS NPs were determined by inductively coupled plasma atomic emission spectroscopy (Thermo Fisher, New York, United States). A 915-nm semiconductor laser (Thorlabs, United States) could be adjusted externally (0–2 W). Calibration of the output power of lasers was conducted by using a handheld optical power meter (OLP-35, VIAVI, United States). To measure the photothermal property, 100 μl of CuS NPs at different concentrations were irradiated with a 915-nm semiconductor laser device at a power density of 0.5 W cm^{-2} for 5 min. To evaluate the photostability of CuS NPs, the solution was irradiated with a 915-nm laser for 5 min, followed by natural cooling without irradiation for 5 min. The procedure was repeated five times. The temperature was recorded

and imaged simultaneously with a thermal imaging camera (FLIR A300, United States).

Cell Culture and Characterization

Raw 264.7 macrophages were cultured in Dulbecco's modified Eagle's medium (4500 mg ml^{-1} glucose), supplemented with 10% fetal bovine serum and 1% streptomycin/penicillin, and maintained at 37°C in a humidified 5% CO_2 atmosphere. The Raw 264.7 macrophages were stained with CD68 and DAPI and observed using a fluorescence microscope (Olympus, Japan).

Cytotoxicity, Cell Viability Assay, and Intracellular Transmission Electron Microscopy

To evaluate the cytotoxicity properties of CuS NPs on macrophages in the absence of PTT, Raw 264.7 was seeded in a 96-well plate (1×10^5 per well) and cocultured with CuS NPs at different concentrations (0, 20, 40, 80, 120, 200, 400, and 800 μg ml^{-1}) for 12 h. CCK-8 cell proliferation assay was conducted to measure the viability of macrophages after cocultured with CuS NPs according to the manufacturer's instructions. Then, the safe concentration of CuS NPs was confirmed and used for the subsequent experiments. To assess the photothermal effects of CuS NPs, Raw 264.7 was cocultured with CuS_2 NPs at safe concentration for 12 h and then irradiated with a 915-nm NIR laser at different power densities (0, 0.3, 0.5, and 1.0 W cm^{-2}). After that, the irradiated macrophages were stained with calcein AM/PI to discriminate living and dead cells (Calcein AM-green fluorescence, PI-red fluorescence) and observed using an inverted fluorescence microscope (Olympus, Japan). For the intracellular TEM, CuS NPs engulfed by macrophages were observed using an intracellular transmission electron microscope (TEM; JEM-1450, Tokyo, Japan).

Animal Model and Photothermal Therapy

Male, 8-week-old apolipoprotein E knockout mice were enrolled in the present study. The animal protocol was approved by the Ethics Review Committee for Animal Experimentation of Shanghai Ninth People's Hospital, Shanghai Jiao Tong University School of Medicine.

The mice were anaesthetized by intraperitoneal injection of 40 mg/kg pentobarbital sodium, and then the left common carotid artery was skeletonized. The LCA was blocked by cross-clamping at the proximal end, and an incision was then made at the distal end of the LCA. A 29G needle (BD Insulin Syringe Ultra-Fine®) was inserted to the LCA, rotated, and pushed forward and backward for three times. After closing the incision, left carotid arteries were wrapped with a constrictive silica collar. After 14 days, 100 μl (80 μg ml^{-1}) CuS NPs were injected into the constrictive silica collar under the guidance of small animal ultrasonic instrument, while the contralateral right carotid arteries were sham-operated to serve as the intra-animal control. The procedure is shown in **Supplementary Figure S1**. Then, 12 h after injection, all groups were subjected to 915-nm NIR laser irradiation at a power density of 0.5 W cm^{-2} for 5 min.

In Vivo Computed Tomography

Small animal CT scanning (SkyScan1278, Brooke, German) was used to determine the imaging property of CuS NPs. The operated mice (intra-collar injection with 100 μl of CuS NPs, 80 μg ml^{-1}) were subjected to CT scanning. 3-dimensional CT imaging was reconstructed to track the distribution of CuS NPs around the LCA.

Histological Analysis and Blood Examination

On the 14th day after PTT, all the mice were sacrificed for histopathological examination. Both collared and sham-operated carotid arteries were harvested. The arteries were stained with macrophage surface marker CD68 and DAPI, and the immunofluorescent signal was detected by using a microscope which was further quantified by ImageJ 1.8.0 software. The number of cells of CD68-positive macrophages was then counted by two investigators who were blinded to group information. The thickness of the intima and media of the arteries was observed by using a microscope after routine HE staining of slides from the carotid arteries and calculated by ImageJ 1.8.0. To observe the restoration of integrity and continuity of the post-injury endarterium, Evans blue staining was performed following the standard protocol.

To assess the *in vivo* toxicity and biocompatibility of CuS NPs, the major viscera, heart, liver, spleen, lung, kidney, and intestine were made to 4- to 6-nm sections for HE staining, and the histopathological changes were observed. Seven age-matched healthy mice were sacrificed as control. All the bloods biochemical parameters were measured in Shanghai Ninth People's Hospital Research Center for Model Organisms.

Statistics Analysis

Parametric data are represented as means ± standard deviation, and comparisons among groups were analyzed by one-way analysis of variance followed by Bonferroni correction for *post hoc* test. The number of macrophages was analyzed by using the Kruskal–Wallis test with Bonferroni correction. P-value <0.05 was considered statistically significant. All data are representative of at least three independent experiments. SPSS, version 25.0 (IBM-SPSS, Inc., Armonk, NY), was used to perform statistical analysis. The comparison results between groups labeled with * for $p < 0.05$ and ** for $p < 0.01$.

RESULTS AND DISCUSSION

Synthesis and Characterization of CuS Nanoparticles

Hydrophilic CuS NPs were prepared by a one-step hydrothermal synthesis method in the presence of sodium citrate. The crystal phase of the products is characterized by using an X-ray diffractometer (XRD). **Figure 1A** shows the XRD pattern of the as-synthesized products. The pattern of the sample can be matched well with the hexagonal CuS phase (JCPDS no. 43-1473), with no other peaks. EDS analysis (**Supplementary Figure S2**) showed that the products were composed of two elements (Cu and S), indicating the high purity of

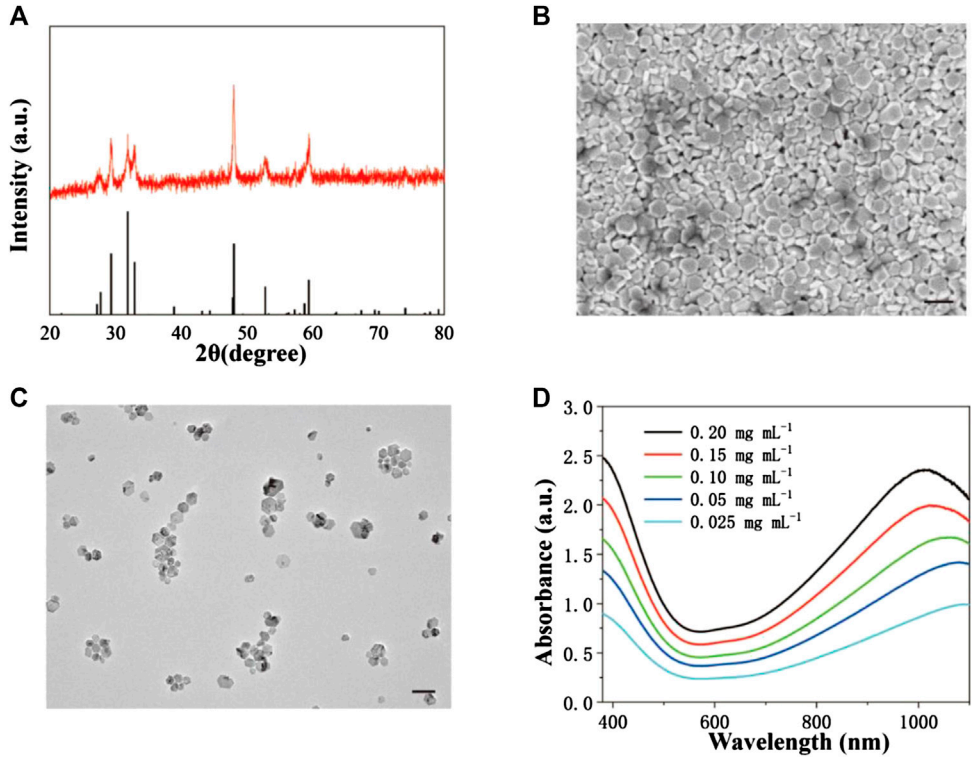

FIGURE 1 | Synthesis and characterization of CuS NPs. **(A)** XRD pattern of CuS NPs. **(B)** SEM image of CuS NPs. Scale bar: 50 nm. **(C)** TEM image of CuS NPs. Scale bar: 50 nm. **(D)** UV-vis-NIR absorption spectrum of CuS NPs at room temperature.

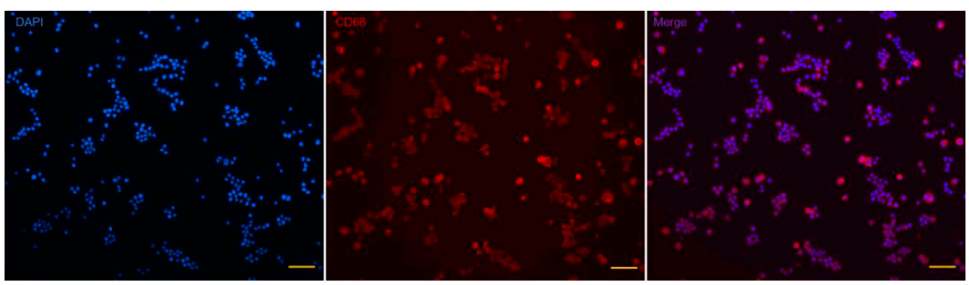

FIGURE 2 | Identification specific surface antigen of Raw 264.7. Nuclear is stained with DAPI (blue); specific surface antigen is positive for CD68 (red). Scale bar: 100 μm.

the CuS NPs. As shown in **Figures 1B,C**, SEM and TEM images confirmed that the products were nanoparticles with a size of 50 nm, showing good dispersion. **Figure 1D** exhibits the UV-vis absorbance spectrum of the aqueous dispersion of CuS NPs. It showed an intense absorption band centered at 1,010 nm. The strong NIR absorption made the CuS NPs an ideal candidate as PTT agents.

Identification of Macrophages and Intracellular Uptake

As an important member of the mononuclear phagocytic system, macrophages own the characteristics of strong phagocytosis and rapid growth. Raw 264.7 has been widely applied to study the function and characteristics of macrophages. Raw 264.7 was identified by cell immunofluorescence to determine the specific surface antigen of macrophages. Cellular immunofluorescence (**Figure 2**) demonstrated that Raw 264.7 was positive for CD68 (red), and nuclear staining with DAPI (blue).

Macrophages are known to be the principal participants in the chronic remodeling of the arterial wall. To detect the possibility of applying PTT using CuS NPs in ablating macrophages, we evaluated the phagocytosis of macrophages toward the CuS NPs using TEM. The intracellular TEM images

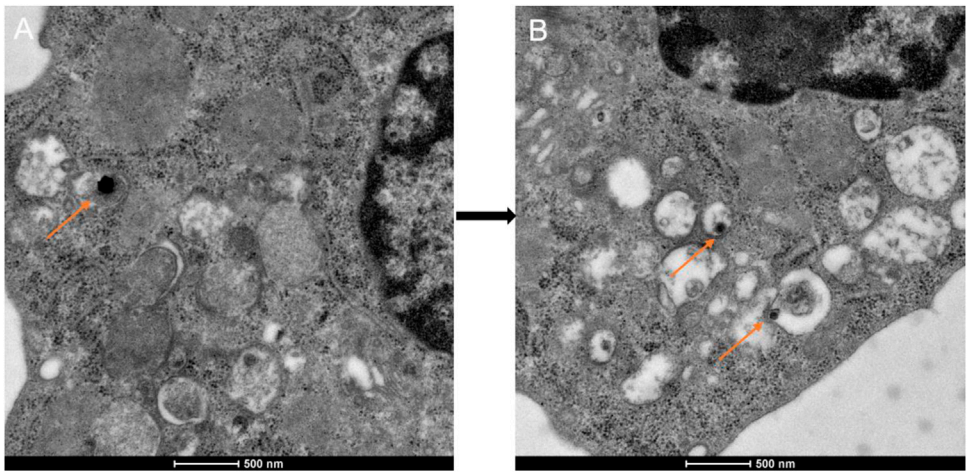

FIGURE 3 | Representative TEM images of phagocytosis of the CuS NPs. **(A)** Raw 264.7 incubated with the CuS NPs for 12 h. **(B)** Karyolysis and cytolysis of Raw 264.7 after incubation with the CuS NPs for 12 h and NIR laser for 5 min at a power density of 0.5 W cm^{-2}. The orange arrows indicate the CuS NPs engulfed by lysosomes.

of Raw 264.7 showed efficient phagocytosis toward the CuS NPs without obvious damage to organelles (**Figure 3A**). However, after coculturing with CuS NPs at a concentration of 80 μg ml^{-1} for 12 h and then undergoing 915-nm NIR laser irradiation at a power density of 0.5 W cm^{-2} for 5 min, significant blebbing, karyolysis, and cytolysis were observed (**Figure 3B**), all indicating that macrophages were induced to apoptosis and/or necrosis after PTT treatment. Thus, the present PTT using CuS NPs as photothermal agents demonstrates a potential application for ablating macrophages to alleviate chronic inflammation.

Cytotoxicity and Photothermal Effect of the CuS Nanoparticles on Macrophages

To evaluate the photothermal effect of CuS NPs, the temperature evolution at different CuS NP concentrations (0, 20, 40, and 80 μg ml^{-1}) under continuous 915-nm wavelength laser irradiation for 300 s was recorded, showing that the temperature elevated in a dramatic and smooth pattern with increment of CuS NP concentration (**Supplementary Figure S3**). Biomedical safety is prerequisite for any clinical application, and the cytotoxicity of the CuS NPs should be assessed. After incubating with the CuS NPs for 12 h, the CCK-8 assay was conducted to detect the concentration-dependent cytotoxicity of the CuS NPs on Raw 264.7. No significant difference was observed in cell viability at the concentrations under 80 μg ml^{-1}. When the concentration reached 120 μg ml^{-1}; the viability of Raw 264.7 was slightly affected (**Figure 4A**). Therefore, CuS NPs below a concentration of 80 μg ml^{-1} were selected for being cocultured with macrophages in subsequent *in vitro* and *in vivo* experiments.

To study the photothermal effect of CuS NPs on macrophages, Raw 264.7 was cocultured with CuS NPs of 80 μg ml^{-1} for 12 h and then exposed to 915-nm laser at different power densities (0, 0.25, 0.5, and 1.0 W cm^{-2}) for 5 min. The CCK-8 assay was conducted to detect the power density–dependent cytotoxicity of the CuS NPs on Raw 264.7. The viability of Raw 264.7 reduced slightly at a power density of 0.25 W cm^{-2}. However, when the power density reached 0.5 W cm^{-2}, the viability of Raw 264.7 reduced markedly (**Figure 4B**). Considering the results above, laser power (0.5 W cm^{-2}) was chosen to mimic the treatment *in vitro*.

Next, Raw 264.7 was incubated with CuS NPs of 80 μg ml^{-1} for 12 h and then exposed to 915-nm laser (0.5 W cm^{-2}) for 5 min. Subsequently, Raw 264.7 cells were stained with calcein AM/PI for discriminating living (green) cells and dead (red) cells. Calcein AM/PI results (**Figure 4C**) showed that no dead cells were observed in the control group (**Figure 4C,a**), and about 25% were dead cells in the CuS NPs group (**Figure 4C,b**), while about 95% cells were dead in the CuS NPs + PTT group (**Figure 4C,c**). The CCK-8 assay showed results consistent with calcein AM/PI results (**Figure 4C,d**). Those results demonstrated that PTT using CuS NPs as NIR absorption agents could eliminate macrophages effectively and may provide great potential to alleviate arterial stenosis.

As an important type of programmed cell death, apoptosis could be induced by the thermal effect of nanoparticles; however, whether it is involved in CuS-based PTT-induced macrophage death is currently unknown. To this end, we performed annexin V/PI staining of macrophages from control, CuS NPs, and CuS NPs + PTT groups, and the flow cytometry analysis showed that the necrosis index of macrophages was slightly higher in the CuS NPs group than in the control group and difference in the apoptosis index was not found between the two groups. In contrast, the CuS NPs + PTT group exhibited a significantly higher either early apoptosis (24.9% vs. 1.97%) or mid/late apoptosis (32.5% vs. 0.76%) index of macrophages than the CuS NPs group (**Figure 5**). However, the necrosis index of the macrophages was similar between CuS NPs and CuS NPs + PTT

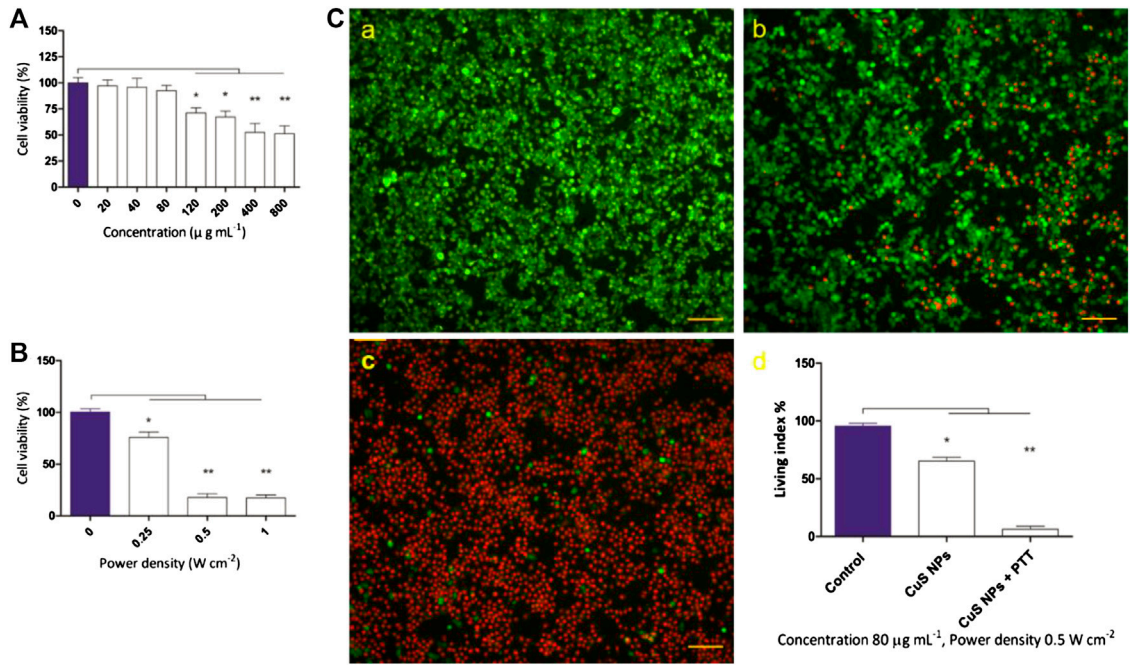

FIGURE 4 | Cytotoxicity of CuS NPs and its thermal effect on macrophages. **(A)** The cell viability of macrophages after cocultured with different concentrations of CuS NPs. **(B)** The cell viability of macrophages cocultured with CuS NPs (80 μg ml^{-1}) exposed to 915 nm NIR laser at different power density for 5 min. **(C)** Representative images of live (green) and dead (red) cells with CuS NPs (80 μg ml^{-1}, 0.5 W cm^{-2}) in the control group, CuS NPs group, CuS NPs + PTT group, respectively. Scale bar: 100 μm.

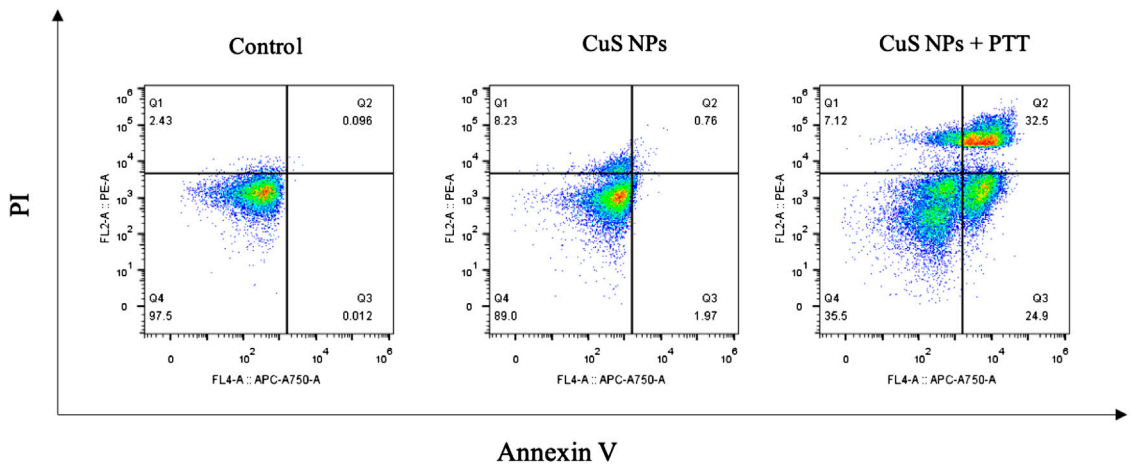

FIGURE 5 | Annexin V/PI duostaining of macrophages. CuS NPs + PTT group exhibited a significantly higher either early apoptosis (Q3) or mid/late apoptosis (Q2) index of macrophages than the CuS NPs group.

groups, indicating that the macrophage cell death induced by the CuS NPs–based photothermal effect was mainly apoptosis, rather than necrosis.

In Vivo Computed Tomography Imaging

In addition to their powerful therapeutic effect, the imaging function of nanomaterials has drawn great attention. Targeted delivery of imaging nanomaterials provides a promising approach for precious location of lesions and accurate diagnosis of diseases (Ge et al., 2020). The binding of Cu^{2+} to black phosphorus not only enhances photothermal stability and accelerates degradation, which makes Cu^{2+}-based nanomaterials the best photothermal agents (Wicki et al., 2015) but also provides *in vivo* real-time and quantitative tracking positron emission tomography–computed tomography (PET-CT) imaging (Hu K. et al., 2020). Moreover, it was reported that

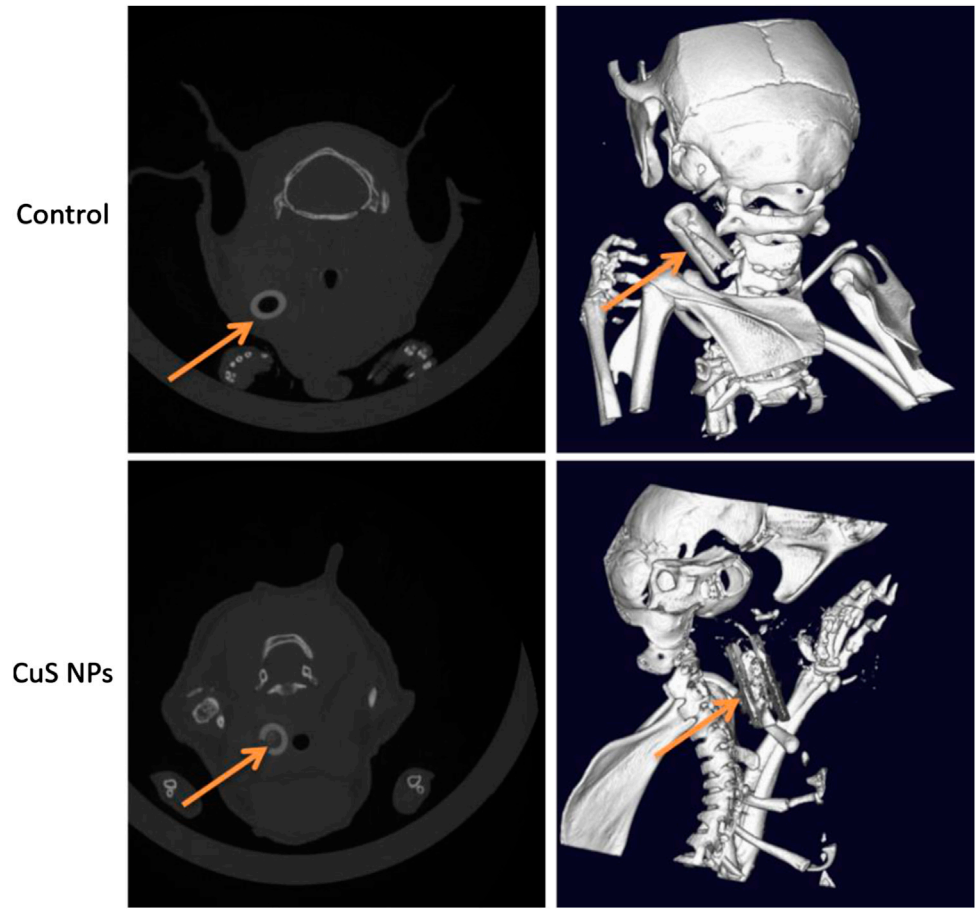

FIGURE 6 | Demonstration of 2D-CT and 3D-CT imaging property of CuS NPs *in vivo*. The orange arrows indicate the CuS NPs and the constrictive silica collars.

chelator-free ^{64}CuS nanoparticles are suitable for PET-CT imaging and robust photothermal ablation (Zhou et al., 2010). In the progression of atherosclerosis, increased accumulation of ^{64}Cu-labeled vMIP-II comb was confirmed by PET-CT imaging and was consistent with histopathological characterization of plaque including increased macrophage number and enlarged size (Luehmann et al., 2016). Collective data have indicated that Cu-based nanomaterials are suitable for CT imaging of tumor and inflammation. As demonstrated in 2D-CT and 3D-CT (**Figure 6**), flocculent and high-density imaging of CuS NPs was confined in the constrictive silica collar that wrapped the common carotid artery, indicating excellent CT imaging property of CuS NPs. Moreover, only little diffusion of CuS NPs to the surrounding tissues and organs was observed, which indicates that the CuS NPs can be accurately located around the lesion and play a role in PTT without causing any side effect.

Photothermal Effect on Carotid Artery Inflammation Induced by Mechanical Injury to Endarterium

PTA or stent implantation in mechanical injury to the endarterium is inevitable (Ng et al., 2017). Post-injury platelet/endothelium interaction promotes penetration of circulating monocytes through the injured endarterium with the regulation of cytokines (Arakawa et al., 2005), microRNAs (Gareri et al., 2016), and adhesion molecules (Hytonen et al., 2016), resulting in the transformation from monocytes to macrophages. Accumulating evidence indicate that activated macrophages surrounding the arterial wall triggers an overproduction of pro-inflammatory factors, which leads to severe hyperplasia of smooth muscle cells and arterial restenosis (Hoare et al., 2019). Therefore, it is plausible that macrophages are the target of ablation by which PTT using CuS NPs alleviates arterial inflammation after mechanical injury to the endarterium and mediates a protective effect on the endarterium. Apo E knockout mice were used to conduct the endarterium injury model and to mimic the mechanical injury of endovascular treatment. According to different treatment procedures, they were divided into control group, CuS NP group, and CuS NP + PTT group. After 14 days, the left carotid arteries were harvested for HE staining and immunofluorescence staining. The results showed that compared with the control group and the CuS NP group, the number of macrophages in the CuS NP + PTT group reduced greatly (**Figures 7A,B**). This suggests that PTT using CuS NPs

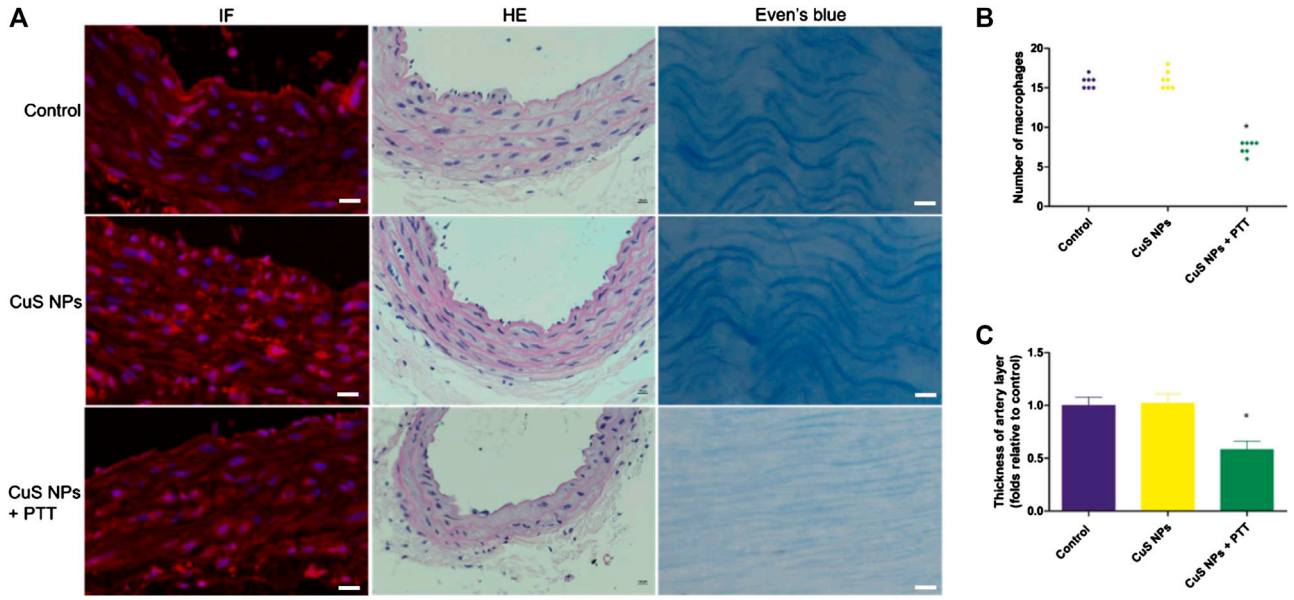

FIGURE 7 | Representative immunofluorescence images of the carotid artery. **(A)** Representative of HE, immunofluorescence (IF) staining, and Evans blue staining of carotid artery from the control group, CuS NP group, and CuS NP + PPT group, respectively. **(B)** Representative of the number of $CD68^{+}$ macrophages in each group. **(C)** Representative of the artery wall thickness in each group. Scale bar: 200 μm.

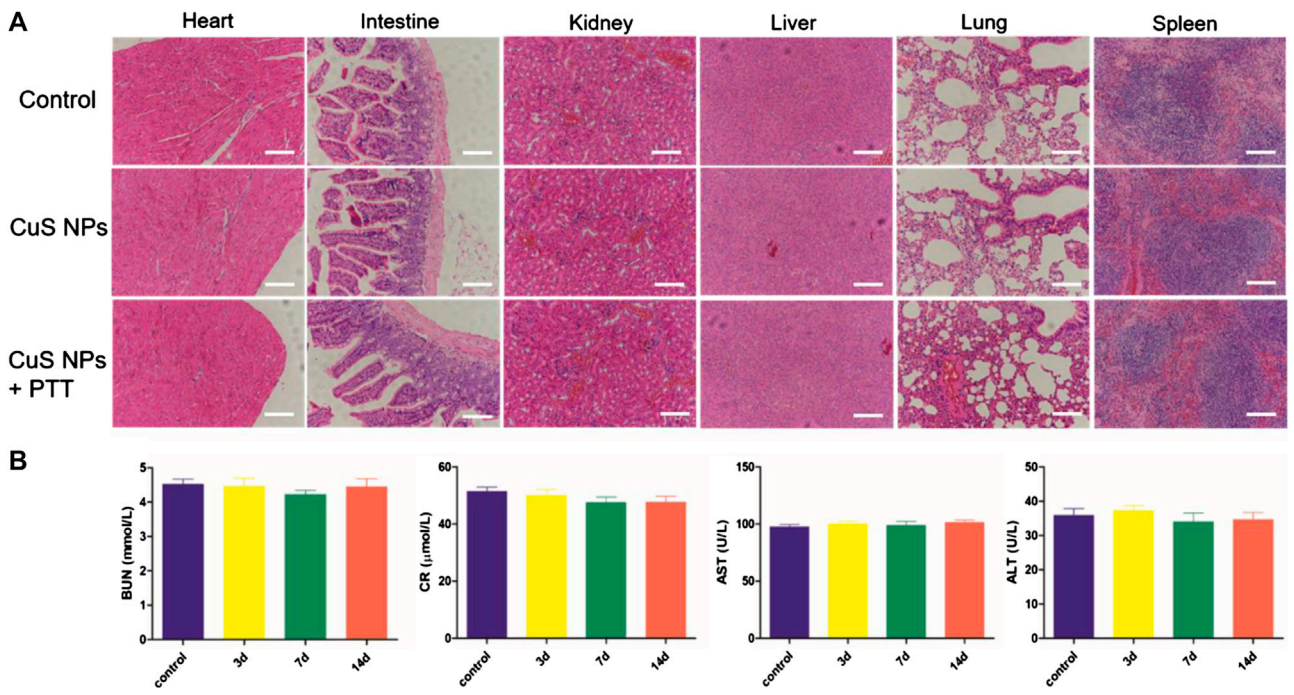

FIGURE 8 | Biocompatibility assay of CuS NPs *in vivo*. **(A)** HE staining of major viscera. No significant pathologic changes were observed in the heart, intestine, kidney, liver, lung, and spleen in the three groups. Scale bar: 200 μm. **(B)** Blood biomedical results of the control group and the CuS NP group at different time points (3, 7, and 14 days) after injection.

can ablate macrophages effectively. What is more, HE staining demonstrated that the thickness of the intima and media in the CuS NP + PTT group was much thinner than that in the control group and the CuS NP group (**Figures 7A,C**). The number of macrophages was revealed to be reduced in the media of the artery in our study, which confirmed the essential role of PTT

using CuS NPs in the ablation of macrophages. Another important finding revealed by the present study was that the thickness of the intima and media was thinnest after the PTT using CuS NPs, which might be associated with 1) apoptosis and necrosis of SMCs induced by higher temperature and 2) inhibition of SMC proliferation through eliminating macrophages. As either percutaneous balloon angioplasty or stent transplantation would unavoidably lead to the injury of the arterial endothelium and endothelial dysfunction, re-endothelialization of the injured arteries after endovascular treatment greatly affects later artery restenosis and patency. Results from Evans blue staining revealed that compared to the control group and the CuS NP group, re-endothelialization of the endarterium in the CuS NP + PTT group restored excellently after PTT as evidenced by more intact and continuous endarterium (**Figure 6A**).

Biocompatibility of the CuS Nanoparticles

Favorable biocompatibility of NPs should be considered and guaranteed for living bodies. Mice from the three groups (n = 7, each) were sacrificed 14 days after PTT, and major viscera were harvested for histopathological examination. Paraffin-embedded sections (4 nm) of major viscera (heart, intestine, kidney, liver, lung, and spleen) were stained with hematoxylin–eosin dye. Compared with the control group, no obvious pathological changes such as cell denaturation and necrosis were observed in the other two groups (**Figure 8A**). Blood samples were tested using the ELISA method. Statistical difference was not found between the three groups in terms of alanine aminotransferase, aspartate aminotransferase, blood urea nitrogen, or creatinine (**Figure 8B**). These results illustrate that CuS NPs as PTT agents have no side effects and are safe for use in the living body.

Limitations

However, several limitations of the work should be merited comment. Macrophage necrosis and apoptosis are the key cellular events in alleviating the negative remodeling of post-injury endarterium. It is not known whether photothermal effects against macrophages, rather than other cells, such as fibroblasts or endothelial cells, contribute to the restoration of post-injury endarterium. The mechanisms by which PTT induces macrophage apoptosis have not been investigated fully. Further investigation is needed to identify the signal pathways regulating macrophage apoptosis.

CONCLUSION

In conclusion, nontoxic and biocompatible CuS NPs can be engulfed by macrophages so that efficient photothermal depletion of macrophages was achieved *in vitro* and *in vivo*. Intra-collar injection of CuS NPs exhibits excellent CT imaging property and no diffusion to the surrounding tissue, which provides precise positioning and targeted therapy. The therapeutic effects of CuS NPs based PTT is proved by the decrease in the number of macrophages and arterial intima/media thickness. To our knowledge, this is the first report that CuS NP-based PTT plays an important role in alleviating arterial restenosis by targeting macrophages. The current study further expanded the understanding of CuS NPs as PTT agent against carotid arterial restenosis after endovascular treatment, which may improve the long-term prognosis of ischemic strokes.

DATA AVAILABILITY STATEMENT

The original contributions presented in the study are included in the article/**Supplementary Material**, further inquiries can be directed to the corresponding authors.

ETHICS STATEMENT

The animal study was reviewed and approved by Ethics Review Committee for Animal Experimentation of Shanghai Ninth People's Hospital, Shanghai Jiao Tong University School of Medicine.

AUTHOR CONTRIBUTIONS

XW, KL, and QH and contributed equally to this work. XW, KL, and QH contributed to experimental operations, statistical analysis, and manuscript writing. QZ contributed to the synthesis of CuS nanoparticles and measurement of the morphology features and the photothermal characteristics. XY, XL, and RW contributed to experimental design, manuscript proofreading, and communication.

FUNDING

This work was supported by the National Natural Science Foundation of China (Grant 81701801, 81971712, and 81870346), Clinical Research Program of Ninth People's Hospital, Shanghai Jiao Tong University School of Medicine (JYLJ019) and Shanghai Municipal Health Bureau Project (202040434).

SUPPLEMENTARY MATERIAL

The Supplementary Material for this article can be found online at: https://www.frontiersin.org/articles/10.3389/fmats.2020.591281/full#supplementary-material.

REFERENCES

Arakawa, H., Qian, J. Y., Baatar, D., Karasawa, K., Asada, Y., Sasaguri, Y., et al. (2005). Local expression of platelet-activating factor-acetylhydrolase reduces accumulation of oxidized lipoproteins and inhibits inflammation, shear stress-induced thrombosis, and neointima formation in balloon-injured carotid arteries in nonhyperlipidemic rabbits. *Circulation* 111 (24), 3302–3309. doi:10.1161/CIRCULATIONAHA.104.476242

Beckman, J. A., Ansel, G. M., Lyden, S. P., and Das, T. S. (2020). Carotid artery stenting in asymptomatic carotid artery stenosis: JACC Review topic of the week. *J. Am. Coll. Cardiol.* 75 (6), 648–656. doi:10.1016/j.jacc.2019.11.054

Cheng, L., Wang, C., Feng, L., Yang, K., and Liu, Z. (2014). Functional nanomaterials for phototherapies of cancer. *Chem. Rev.* 114 (21), 10869–10939. doi:10.1021/cr400532z

de Melo-Diogo, D., Pais-Silva, C., Dias, D. R., Moreira, A. F., and Correia, I. J. (2017). Strategies to improve cancer photothermal therapy mediated by nanomaterials. *Adv. Healthc. Mater.* 6 (10), 1700073. doi:10.1002/adhm.201700073

Gareri, C., De Rosa, S., and Indolfi, C. (2016). MicroRNAs for restenosis and thrombosis after vascular injury. *Circ. Res.* 118 (7), 1170–1184. doi:10.1161/CIRCRESAHA.115.308237

Ge, J., Zhang, Q., Zeng, J., Gu, Z., and Gao, M. (2020). Radiolabeling nanomaterials for multimodality imaging: new insights into nuclear medicine and cancer diagnosis. *Biomaterials* 228, 119553. doi:10.1016/j.biomaterials.2019.119553

Hoare, D., Bussooa, A., Neale, S., Mirzai, N., and Mercer, J. (2019). The future of cardiovascular stents: bioresorbable and integrated biosensor technology. *Adv. Sci.* 6 (20), 1900856. doi:10.1002/advs.201900856

Hong, M. K., and Lee, S. Y. (2020). Differential effects of drug-coated balloon angioplasty for in-stent restenosis. *J. Am. Coll. Cardiol.* 75 (21), 2679–2681. doi:10.1016/j.jacc.2020.04.005

Hu, K., Xie, L., Zhang, Y., Hanyu, M., Yang, Z., Nagatsu, K., et al. (2020). Marriage of black phosphorus and Cu(2+) as effective photothermal agents for PET-guided combination cancer therapy. *Nat. Commun.* 11 (1), 2778. doi:10.1038/s41467-020-16513-0

Hu, X., Lu, Y., Zhou, L., Chen, L., Yao, T., Liang, S., et al. (2020). Post-synthesis strategy to integrate porphyrinic metal-organic frameworks with CuS NPs for synergistic enhanced photo-therapy. *J. Mater. Chem. B* 8 (5), 935–944. doi:10.1039/c9tb02597a

Hytonen, J., Leppanen, O., Braesen, J. H., Schunck, W. H., Mueller, D., Jung, F., et al. (2016). Activation of peroxisome proliferator-activated receptor-delta as novel therapeutic strategy to prevent in-stent restenosis and stent thrombosis. *Arterioscler. Thromb. Vasc. Biol.* 36 (8), 1534–1548. doi:10.1161/ATVBAHA.115.306962

Jinnouchi, H., Guo, L., Sakamoto, A., Torii, S., Sato, Y., Cornelissen, A., et al. (2020). Diversity of macrophage phenotypes and responses in atherosclerosis. *Cell. Mol. Life Sci.* 77 (10), 1919–1932. doi:10.1007/s00018-019-03371-3

Koelwyn, G. J., Corr, E. M., Erbay, E., and Moore, K. J. (2018). Regulation of macrophage immunometabolism in atherosclerosis. *Nat. Immunol.* 19 (6), 526–537. doi:10.1038/s41590-018-0113-3

Li, L., Yiin, G. S., Geraghty, O. C., Schulz, U. G., Kuker, W., Mehta, Z., et al. (2015). Incidence, outcome, risk factors, and long-term prognosis of cryptogenic transient ischaemic attack and ischaemic stroke: a population-based study. *Lancet Neurol.* 14 (9), 903–913. doi:10.1016/s1474-4422(15)00132-5

Li, Y., Lu, W., Huang, Q., Huang, M., Li, C., and Chen, W.(2000). Copper sulfide nanoparticles for photothermal ablation of tumor cells. *Nanomedicine (Lond.)* 5 (8), 1161–1171. doi:10.2217/nnm.10.85

Luehmann, H. P., Detering, L., Fors, B. P., Pressly, E. D., Woodard, P. K., Randolph, G. J., et al. (2016). PET/CT imaging of chemokine receptors in inflammatory atherosclerosis using targeted nanoparticles. *J. Nucl. Med.* 57 (7), 1124–1129. doi:10.2967/jnumed.115.166751

Ng, J., Bourantas, C. V., Torii, R., Ang, H. Y., Tenekecioglu, E., Serruys, P. W., et al. (2017). Local hemodynamic forces after stenting: implications on restenosis and thrombosis. *Arterioscler. Thromb. Vasc. Biol.* 37 (12), 2231–2242. doi:10.1161/ATVBAHA.117.309728

Peng, Z., Qin, J., Li, B., Ye, K., Zhang, Y., Yang, X., et al. (2015). An effective approach to reduce inflammation and stenosis in carotid artery: polypyrrole nanoparticle-based photothermal therapy. *Nanoscale* 7 (17), 7682–7691. doi:10.1039/c5nr00542f

Poudel, K., Gautam, M., Jin, S. G., Choi, H. G., Yong, C. S., and Kim, J. O. (2019). Copper sulfide: an emerging adaptable nanoplatform in cancer theranostics. *Int. J. Pharm.* 562, 135–150. doi:10.1016/j.ijpharm.2019.03.043

Qin, J., Peng, Z., Li, B., Ye, K., Zhang, Y., Yuan, F., et al. (2015). Gold nanorods as a theranostic platform for *in vitro* and *in vivo* imaging and photothermal therapy of inflammatory macrophages. *Nanoscale* 7 (33), 13991–14001. doi:10.1039/c5nr02521d

Tong, Y., Cai, L., Yang, S., Liu, S., Wang, Z., and Cheng, J. (2020). The Research progress of vascular macrophages and atherosclerosis. *Oxid. Med. Cell Longev.* 2020, 7308736. doi:10.1155/2020/7308736

Wang, J., Wu, X., Shen, P., Wang, J., Shen, Y., Shen, Y., et al. (2020). Applications of inorganic nanomaterials in photothermal therapy based on combinational cancer treatment. *Int. J. Nanomedicine* 15, 1903–1914. doi:10.2147/IJN.S239751

Wang, X., Wu, X., Qin, J., Ye, K., Lai, F., Li, B., et al. (2019). Differential phagocytosis-based photothermal ablation of inflammatory macrophages in atherosclerotic disease. *ACS Appl. Mater. Interfaces* 11 (44), 41009–41018. doi:10.1021/acsami.9b12258

Wicki, A., Witzigmann, D., Balasubramanian, V., and Huwyler, J. (2015). Nanomedicine in cancer therapy: challenges, opportunities, and clinical applications. *J. Control Release* 200, 138–157. doi:10.1016/j.jconrel.2014.12.030

Williams, J. W., Huang, L. H., and Randolph, G. J. (2019). Cytokine circuits in cardiovascular disease. *Immunity* 50 (4), 941–954. doi:10.1016/j.immuni.2019.03.007

Yang, W., Guo, W., Le, W., Lv, G., Zhang, F., Shi, L., et al. (2016). Albumin-bioinspired Gd:CuS nanotheranostic agent for in vivo photoacoustic/magnetic resonance imaging-guided tumor-targeted photothermal therapy. *ACS Nano* 10 (11), 10245–10257. doi:10.1021/acsnano.6b05760

Zhang, X., Liu, J., Yang, X., He, G., Li, B., Qin, J., et al. (2019). CuCo2S4 nanocrystals as a nanoplatform for photothermal therapy of arterial inflammation. *Nanoscale* 11 (19), 9733–9742. doi:10.1039/c9nr00772e

Zhou, M., Zhang, R., Huang, M., Lu, W., Song, S., Melancon, M. P., et al. (2010). A chelator-free multifunctional [64Cu]CuS nanoparticle platform for simultaneous micro-PET/CT imaging and photothermal ablation therapy. *J. Am. Chem. Soc.* 132 (43), 15351–15358. doi:10.1021/ja106855m

Conflict of Interest: The authors declare that the research was conducted in the absence of any commercial or financial relationships that could be construed as a potential conflict of interest.